

# Fine control of hypocotyl elongation through COP1-dependent COL3-COL13 feedback pathway

Bin Liu<sup>1</sup>, Hong Long<sup>2</sup>, Jing Yan<sup>2</sup>, Lili Ye<sup>2</sup>, Qin Zhang<sup>2</sup>, Hongmei Chen<sup>2</sup>, Sujuan Gao<sup>2</sup>, Yaqin Wang<sup>2</sup>, Xiaojing Wang<sup>3</sup>, and Shulan Sun<sup>3</sup>

<sup>1</sup>Shanghai Jiao Tong University - Minhang Campus

<sup>2</sup>South China Normal University

<sup>3</sup>Guangdong Provincial Key Lab of Biotechnology for Plant Development

May 5, 2020

## Abstract

CONSTANS-LIKE (COL) family members are commonly implicated in light signal transduction during early photomorphogenesis. However, some of their functions remain unclear. Here we propose a role for COL13 on the hypocotyl elongation in *Arabidopsis thaliana*. We found that COL13 RNA accumulates to high levels in hypocotyl, and that disruption of COL13 function via T-DNA insertion or RNAi led to longer hypocotyl of *Arabidopsis* seedlings in red light. On the contrary, overexpression of COL13 resulted in shorter hypocotyl. With various genetic, genomic and biochemical assays, we proved that another COL protein named COL3 directly bound to the promoter of COL13, and the promoter region of COL3 was targeted by the transcription factor LONG HYPOCOTYL 5 (HY5), to form a HY5-COL3-COL13 regulatory chain for regulating hypocotyl elongation in red light. In addition, further study demonstrated that COL13 interacted with COL3 and COL13 promoted the interaction between COL3 and CONSTITUTIVE PHOTOMORPHOGENIC1 (COP1), suggesting a possible COP1-dependent COL3-COL13 feedback pathway. Our results provides new information regarding the genes network in mediating hypocotyl elongation.

## Introduction

Light is one of the most important environmental cues influencing the early stages of post-germination plant development (Kami, Lorrain, Hornitschek, & Fankhauser, 2010; Olle & Viršile, 2013; G. Wu, Cameron, Ljung, & Spalding, 2010). Light-grown seedlings exhibit a developmental response termed photomorphogenesis, resulting in short hypocotyls and expanded, green cotyledons. By contrast, dark-grown seedlings are characterized by long hypocotyls and unexpanded, etiolated cotyledons; this process is called skotomorphogenesis (Josse & Halliday, 2008; McNellis & Deng, 1995; Smith, 2000). As a central light signal repressor, the RING finger protein *CONSTITUTIVE PHOTOMORPHOGENIC1* (COP1) is involved in many light-regulated responses and is responsible for the ubiquitination and degradation of several positive transcription factors in the dark (Dornan et al., 2004; Duek, Elmer, van Oosten, & Fankhauser, 2004; Lau & Deng, 2012; Osterlund, Hardtke, Wei, & Deng, 2000; Seo, Watanabe, Tokutomi, Nagatani, & Chua, 2004; Seo et al., 2003). For example, COP1 interacts with ELONGATED HYPOCOTYL 5 (HY5), which is a positive regulator under far-red, red, blue, and UV-B light conditions (Ang et al., 1998; Delker et al., 2014; Hardtke et al., 2000); COP1 also interacts with CONSTANS-LIKE3 (COL3), which acts as a positive regulator in red light and localizes to nuclear speckles. In addition, the *col3* mutant partially suppresses the *cop1* mutation, suggesting that COL3 acts genetically downstream of COP1 (Datta, Hettiarachchi, Deng, & Holm, 2006).

The loss-of-function *col3* mutant has longer hypocotyls, flowers early and shows a reduced number of lateral branches (Datta et al., 2006). COL3 also directly interacts with B-BOX32 (BBX32), which is regulated by

the circadian clock, to mediate flowering (Tripathi, Carvallo, Hamilton, Preuss, & Kay, 2017). Interestingly, both COL3 and BBX32 belong to the BBX zinc finger transcription factor (TF) family, which has 32 members (Kumagai et al., 2008). This gene family is divided into five groups based on whether their respective proteins contain one or two BBX motifs and whether or not they possess a CCT domain (Khanna et al., 2009). BBX family members, some of which have been characterized (Cheng & Wang, 2005; Graeff et al., 2016; Li et al., 2014; Park et al., 2011; Preuss et al., 2012; Wang, Guthrie, Sarmast, & Dehesh, 2014; Xu, Jiang, Li, Holm, & Deng, 2018; Xu et al., 2016; Yang et al., 2014), are commonly implicated in light signal transduction during early photomorphogenesis. The first BBX protein to be identified in *Arabidopsis thaliana* was CONSTANS (CO) (Putterill, Robson, Lee, Simon, & Coupland, 1995). In addition to CO, 16 other CO-Like (COL) proteins have been identified, which contain one or two B-box domains at the N-terminus and a CCT domain at the C terminus (Cheng & Wang, 2005). However, most of their functions remain unclear.

A previous study showed that COL3 plays multiple roles in plant development (e.g. flowering, hypocotyl elongation and lateral root formation) (Datta et al., 2006). Although COL3 is known to interact with B-BOX32 to regulate flowering (Tripathi et al., 2017), there has been little research on how COL3 regulates hypocotyl elongation and the respective downstream pathways are uncharacterized. In the present study, we propose a role for COL13/B-BOX11 and a possible COP1-dependent COL3-COL13 feedback pathway in regulating the hypocotyl growth in *A. thaliana*.

## Materials and methods

### Plant materials and growth conditions

The *A. thaliana* mutant *col13* (GK657F04-023194) in the Columbia background (Col-0) was bought from Germany (GABI-Kat, Max Planck Institute for Plant Breeding Research, Carl-von-Linné-Weg 10, 50829 Köln, Germany) (Rosso et al., 2003), while *col3* was generously provided by Professor Magnus Holm (Datta et al., 2006). Col-0, Ws and their F1 hybrid were used as wild-type controls. Seed sterilization and growth were as previously described in our paper (B. Liu et al., 2016).

### Hypocotyl Experiments

The light-response assays were performed as previously with some changes (Datta et al., 2006). Plates were 4°C treated for 72 hours and then moved to white light for 10 h to induce uniform germination. After that, the plates were transferred to different light conditions (Dark, white, red and blue light) and incubated at 22 for 3-6 d for hypocotyl measurement. Red and blue lights were generated by light emission diodes at 670 and 470 nm, respectively (model E-30LED; Percival Scientific). The light intensity is around 100  $\mu\text{mol}/\text{m}^2 \cdot \text{s}$  ppfd. The hypocotyl lengths of seedlings were measured/counted using ImageJ software.

### Plasmid construction

Constructs for overexpression and RNAi assays: To make the *COL13* overexpression construct, the predicted full-length *COL13* cDNA was cloned and inserted into the pCAMBIA1390 vector between the *Sal* I and *Eco* RI restriction sites. To generate the *COL13* -RNAi transgenic plants, two fragments of the *COL13* coding sequence were amplified by PCR using primers containing *Pst* I (5' end) and *Mlu* I (3' end) restriction sites, and *Hin* dIII (5' end) and *Bam* HI (3' end) restriction sites. The two fragments were inserted into the pRNAi-0 vector in the reverse orientation.

Constructs for GUS staining assays: To make the p*COL13* -GUS-2000 construct, a region comprising the 2000 bp promoter sequence of *COL13* was cloned and inserted into the pBI121 vector between the *Hin* dIII and *Bam* HI sites. To make the p*COL13* -GUS-2812 construct, a region comprising the 2812 bp promoter sequence of *COL13* was cloned and inserted into the 1301 vector between the *Sac* I and *Sal* I sites. To make the p*COL3* -GUS construct, a region comprising the 967 bp promoter sequence of *COL3* was cloned and inserted into the pBI101 vector between the *Hind* III and *Xba* I sites.

Constructs for yeast assays: To make the *COL3* -pGBKT7, *COP1* -pGBKT7, *COL13* -pGBKT7, *COL3* -pGADT7, *COP1* -pGADT7 and *COL13* -pGADT7 constructs, the *COL3*, *COP1* and *COL13* fragments were

subcloned into the pGBKT7 vector (Gal4 DNA binding domain, Cat. No. 630489, Clontech) and pGADT7 (Gal4 activation domain, Cat. No. 630442, Clontech), as appropriate. To make the COL3-pBbidge and COL3-COL13-pBbidge constructs, the *COL3* and *COL13* fragments were subcloned into the pBbidge<sup>TM</sup> vector (Cat. No. 630404, Clontech) as appropriate.

Constructs for GFP, CFP and YFP assays: To make the *COL13* -GFP construct, the full-length *COL13* coding region was cloned and inserted into the pBEGFP vector between the *Xba* I and *Kpn* I restriction sites. To make the COL3-CFP, COP1-CFP, COL13-CFP, COL3-YFP, COP1-YFP and COL13-YFP constructs, the full-length coding regions of *COL3*, *COP1* and *COL13* were cloned and inserted into the pBluescript II Phagemid vector (Y. Liu et al., 2016), as appropriate.

Constructs for CO-IP assays: To make the 35S:*COL3*- HA construct, the full-length *COL3* cDNA was cloned and inserted into the pCAMBIA1390-HA vector.

Constructs for dual-luciferase assays: Fragments of the COL3 or COL13 promoter were cloned into pGREEN0800-LUC to generate reporter vectors. A modified pBluescript vector (pBS) was used as an effector (Han et al., 2017).

The primers used are listed in Supplementary Table 1.

### Plant transformation

Constructs in binary vectors were introduced into *Agrobacterium tumefaciens* strain LBA4404 and transformed into *Arabidopsis* WT or mutant plants by the floral-dip method (Clough & Bent, 1998). Approximately 30 T1 transgenic plants for each transgene were screened on MS medium supplemented with the appropriate antibiotics, and phenotypic analyses were performed in T2 or later generations.

### Semi-quantitative PCR and qPCR

Semi-quantitative PCR and qPCR analyses were performed as previously described (Zhang, Liu, et al., 2014). RNA was extracted from 5-days young seedlings. Three biological as well as three technical repetitions were performed for each combination of cDNA samples and primer pairs. The primers used are listed in Supplementary Table 1.

### Dual-luciferase assay

Protoplasts were isolated and the dual-luciferase assay was performed as our previously described paper (Han et al., 2017). Transformed protoplasts were incubated at room temperature for 20-22 h, and luciferase activities were measured using the dual-luciferase assay system (Dual-Luciferase Reporter Assay, Promega, United States) according to the manufacturer's instructions. Firefly luciferase activity was normalized to Renilla luciferase activity. Three biological replicates were performed for all experiments.

### Electrophoretic mobility shift assay (EMSA)

EMSA was performed as our previously described paper with the LightShift Chemiluminescent EMSA kit (Thermo Scientific, United States) (Han et al., 2017). The dual-luciferase assay mapped the COL3 binding site to a 1059-bp region of the *COL13* promoter, that located between 676 and 1675 bp upstream of the transcription start site (ATG) (Fig. 5b). This promoter region was used as a 5' end biotin labeled probe and the same fragment, but unlabeled, was used as a competitor. To investigate core-binding motif of the 1059-bp region, a series of EMSAs involving deletions of this region were done. We divided the 1059-bp promoter sequence into five overlapping regions: -1675 to -1391 bp (probe 1), -1421 to -1184 bp (probe 2), -1201 to -1040 bp (probe 3), -1060 to -868 bp (probe 4), and -898 to -616 bp (probe 5). The sequence of probes are listed in Supplementary Table 2.

### Yeast assays

The yeast two-hybrid and three-hybrid assay were performed using a Clontech kit (PT3024-1 (PR973283)). For yeast two-hybrid assays, the bait vectors (pGBKT7 plus candidate genes) and prey vectors (pGAGT7

plus candidate genes) were transformed to Gold and Y187 yeast strain, respectively, then pick each one colony of them to do the mating, and spray the mating solution on SD/-Trp/-Leu/X- $\alpha$ -Gal/AbA (DDO/X/A) agar plates, the positive results were confirmed by growing them on SD/-Ade/-His/-Trp/-Leu/X- $\alpha$ -Gal/AbA (QDO/X/A) agar plates. For yeast three-hybrid assay, COP1-pGADT7 and COL3-COL13-pBbidge constructs were co-transformed into Gold yeast strain. Pick each colony and grow them in SD/-Leu/-Met/-Trp and SD/-Leu/-Trp solution, respectively. Normalized Miller Units were calculated as a ratio of  $\alpha$ -galactosidase activity in yeast. For all yeast assays, we used empty vector as controls.

### Co-immunoprecipitation (CO-IP)

CO-IP were performed as previously described (Fiil, Qiu, Petersen, Petersen, & Mundy, 2008). 35S:COL3-HA and 35S:COL13-GFP constructs were transformed into EHA105 *Agrobacterium* cells and then used to generate 35S:COL3-HA and 35S:COL3-HA::COL13-GFP transgenic plants. Proteins were extracted from 18-d-old seedlings.

### Histochemical GUS staining, GFP, and FRET experiments

Histochemical GUS staining, GFP microscopy and FRET were performed as previously described with some changes (Datta et al., 2006; Hou, Wu, & Gan, 2013; Zhang, Zhang, et al., 2014).

For GUS staining assay, the young seedlings (4 days after germination) were fixed and incubated in GUS-staining solution for 24 h at 37°C. Stained samples were then cleaned with 75% ethanol and observed by dissecting microscope.

For GFP assay, the fusion *COL13*-GFP constructs were transformed into protoplast for transient expression as previously described (F.-H. Wu et al., 2009). Ten stable transgenic plants with *COL13*-GFP were obtained by the floral-dip method. The photos of GFP were taken by confocal microscope Olympus.

For FRET assay, images were acquired using an Olympus confocal microscope, protoplasts were visualized 16 h after transforming. The CFP was excited by a laser diode 405 laser and the YFP by an argon-ion laser. The target regions were bleached with 100 iterations by the argon-ion laser at 100%.

### Statistical analysis

Experimental data were analyzed using ANOVA, and the statistical significance of any differences between treatments was tested using Duncan's test or t-tests. All analyses were carried out using the SPSS for window.

## Results

### *COL13* RNA accumulates to high levels in hypocotyls

By searching the gene expression information in The Arabidopsis Information Resource (TAIR) database (Klepikova, Kasianov, Gerasimov, Logacheva, & Penin, 2016), we found that *COL13*(*AT2G47890*) highly expressed in hypocotyl. Quantitative PCR (qPCR) analysis confirmed that *COL13* were expressed in most plant organs, with a higher expression in hypocotyl and stem (Fig.1a). To determine the spatial patterns of *COL13* expression in more detail, transgenic lines expressing GUS driven by the 2812 bp *COL13* promoter fragment were generated. As shown in Fig.1b, GUS expression was predominantly active in hypocotyl.

### *COL13* regulates hypocotyl elongation under red-light conditions

To characterize the role of *COL13* in plants, we obtained the corresponding *Arabidopsis* T-DNA insertion mutant (GK-657F04-023194, termed *col13* in the following; Fig.S1a) from GABI-Kat, Max Planck Institute for Plant Breeding Research (Rosso et al., 2003); the mutation was verified by PCR (Fig.S1b), which amplify the *sul* gene by using the primers listed in Supplementary Table 1. To confirm that the phenotype of the *col13* mutant was indeed caused by disruption of the *COL13* gene, we generated *COL13* overexpression (OX) (Fig.2a) and *COL13* RNAi transgenic lines (Fig.2b) for comparison.

To examine whether *COL13* is involved in light responses, wild type (WT), *COL13* RNAi and *col13* seedlings were germinated and grown in different light (White, red, blue), as well as dark condition. As shown in

Fig.S1c, under white or red light, the *COL13* RNAi and *col13* seedlings had longer hypocotyls than WT, while in blue light or dark condition, the hypocotyl length of all seedlings were no significant difference. Therefore, our research focus on red light. For further study, *COL13* OX, *COL13* RNAi, *col13* and WT seedlings were germinated and grown in red light. We found that the *COL13*OX seedlings had shorter hypocotyls than WT in red light (Fig. 2c,d), in contrast, the *COL13* RNAi and *col13* seedlings had longer hypocotyls than WT under the same conditions (Fig. 2c, e). These findings suggest that *COL13* acts as a positive regulator of red light-mediated inhibition of hypocotyl elongation.

### Genetic interaction and physiological characterization of hypocotyl elongation

Given that the *phyB*, *hy5*, *col3* and *cop1* mutations can affect hypocotyl elongation under red light conditions (Datta et al., 2006; J. Lee et al., 2007; Peter H Quail, 2002; von Arnim & Deng, 1994), we investigated the expression of *COL13* in the absence of *PHYB*, *COL3*, *HY5* and *COP1*. Semi-quantitative PCR and quantitative PCR (qPCR) analysis revealed that the expression of *COL13* in *phyB*, *col3* or *hy5* knockout plants was significantly reduced compared with that in the WT, while the expression of *COL13* in the *cop1* mutants was increased (Fig. 3a,b). As the expression of *COL13* decreased the most in the *col3* mutant, we generated transgenic lines expressing GUS under control of the *COL13* promoter in the *col3* mutant background. Interestingly, while the *COL13* promoter was active in the hypocotyl as well as cotyledon in WT seedlings, GUS expression was not detected in the hypocotyl in the *col3* mutant background (Fig. 3c).

To understand the functional relationship and genetic interaction between *COL13* and *COL3* and their role in the regulation of hypocotyl growth, we generated a *col13 xcol3* double mutant, and examined hypocotyl length under red light conditions. Given that *col13* is in Col-0 and *col3* is in WS background, crossing lines from different backgrounds very likely will have an effect on the hypocotyl length. To reduce the effect from background, we use the F1 hybrid of Col-0x WS as WT. We found that, while hypocotyl length in the double mutant *col13xcol3* was longer than in WT seedlings, it was not significantly different to hypocotyl length in the single mutants, *col13* or *col3*. (Fig. 3d). To confirm this result, we made the RNAi lines of *COL13* in the *col3* mutant background (Fig. 3e), and we obtained the same result as Fig. 3d. Additionally, we also generated a *COL13* -OX line in the *col3* mutant background, and showed that hypocotyl length in this strain was similar to that of WS, and significantly shorter than that of the *col3* mutant (Fig. 3e). In other words, overexpression of *COL13* rescued the phenotype exhibited by the *col3* mutant. Taken together, our results suggest that *COL13* might be the downstream of *COL3* in the red-light mediated signaling pathway.

### The HY5-COL3-COL13 regulatory chain

Based on the genetic data, *col3 hy5* double mutant behaved like the *hy5* mutation (Datta et al., 2006), and *COL13* might be the downstream of *COL3* in regulating hypocotyl elongation, we hypothesized that there is a HY5-COL3-COL13 regulatory chain for controlling hypocotyl growth. To test this hypothesis, HY5 and *COL3* coding sequence, as well as a deletion series of the *COL13* promoter were cloned into the dual-luciferase system, respectively (Fig. 4a). As shown in Figure 4b, these dual-luciferase experiments confirmed the ability of HY5 to bind to the *COL3* promoter and *COL3* to bind to the *COL13* promoter. In addition, these experiments also map the *COL3* target regions to between -1675 bp and -616 bp of the *COL13* promoter (Fig. 4b). The in vivo interaction of *COL3* with this 1059-bp sequence of the *COL13* promoter was further confirmed by electrophoresis mobility shift assay (EMSA; Fig. 4c). To investigate core-binding motif of the 1059-bp region, a series of EMSAs involving deletions of this region were done. We divided the 1059-bp promoter sequence into five overlapping regions: -1675 to -1391 bp (probe 1), -1421 to -1184 bp (probe 2), -1201 to -1040 bp (probe 3), -1060 to -868 bp (probe 4), and -898 to -616 bp (probe 5), and showed that probe 2 (-1421 to -1184 bp) was essential for binding of *COL3* to the *COL13* promoter (Fig. S2).

### COL13 is located in the nucleus

Transformation of *Arabidopsis* protoplasts with a construct expressing *COL13*-CFP indicated that *COL13* is located in the nucleus (Fig. 5a), and a similar result was obtained when the root apical cells of stable *COL13*-GFP transgenic plants were examined (Fig. 5b).

## COL13 interacts with COL3 , but not COP1

According to previous reports, both COL3 and COL13 are CONSTANS (CO)-like proteins, they are related to CO (Robson et al., 2001), and as shown for COL13 above, COL3 also positively regulates red light-mediated inhibition of hypocotyl elongation in *Arabidopsis* (Datta et al., 2006). We also demonstrated above that COL13 shares the same subcellular localization as COL3 (Fig. 5a, b). Given that COL3 can interact with BBX32 and that COL13 also belongs to the BBX zinc finger TF family, we hypothesized that COL3 might interact with COL13. This idea was supported by a two-hybrid assay revealing that COL3 was able to interact with COL13 protein in yeast (Fig. 6a). Next, we examined the interaction in transgenic plants expressing both COL3 and COL13, and showed that COL13 was co-immunoprecipitated with COL3 from seedling tissues (Fig. 6b). The interaction between COL13 and COL3 was also demonstrated in plant cells in a fluorescence resonance energy transfer (FRET) assay (Fig. 6c-f). As shown in Fig. 6c, both cyan fluorescent protein (CFP)-fused COL3 and yellow fluorescent protein (YFP)-fused COL13 were observed in the nucleus after excitation with a 405-nm or a 514-nm laser, respectively. After bleaching an area of interest with the 514-nm laser, YFP-COL13 fluorescence was reduced dramatically, whereas there was a clear increase in CFP-COL3 emission in the same area (Fig. 6d), indicating that FRET had occurred. The relative intensities of emissions from CFP-COL3 and YFP-COL13 in the area of interest, before and after bleaching, are shown in Fig. 6e,f.

## COL13 promotes the interaction between COL3 and COP1

Interestingly, although COL13 and COL3 have similar structures, containing two N-terminal tandemly repeated B-box domains and a CCT domain in the C-terminal, only COL3 can interact with COP1, COL13 does not bind to COP1 (Fig.6a). The results were also demonstrated by FRET assay (Fig. S3a-h). To investigate if COL13 influences the interaction between COP1 and COL3, we performed a yeast three-hybrid assay. In this yeast system, COL3-COL13-pBridge construct allows expression of the *COL3-BD* /bait and *COL13* in yeast, and *COL13* only expressed in the absence of methionine (Met). As shown in Fig.7a, the growth of yeast carrying indicated constructs on selective medium (+Met or -Met) along with an  $\alpha$ -galactosidase assay showed that COP1 and COL3 had stronger binding activity with the expression of COL13. Based on previous report, COP1 interacted with COL3 and inhibited the production of COL3 (Datta et al., 2006). By combining our results above, we proposed a possible COP1-dependent COL3-COL13 feedback pathway (Fig.7b), which involved in regulation of hypocotyl elongation.

## Discussion

Light regulates plant photomorphogenesis. With a large number of genes which are involved in such photomorphogenesis processes were identified as light receptors (Datta et al., 2006; Kircher et al., 2002; Peter H. Quail, 2002), signal transduction factors (Gangappa et al., 2013; Osterlund et al., 2000) or degradation proteins (Crocco, Holm, Yanovsky, & Botto, 2010; Crocco et al., 2015; Delker et al., 2014), one of the immediate questions is how these genes act in a network to mediate various light-related phenotypes. It has been proved that there were multiple pathways that are interlinked to form a gene network of photomorphogenesis (Lau & Deng, 2012; H.-J. Lee, Park, Ha, Baldwin, & Park, 2017). Among these pathways, it is worth mentioning that the ones formed by a subset of family genes termed COL genes (Cheng & Wang, 2005). These family genes played multiple roles in plant development (Datta et al., 2006; Graeff et al., 2016; Muntha et al., 2018; Tripathi et al., 2017; Wang et al., 2014). As an effort toward COLs networking, we investigated the relationship between *COL3* and *COL13* , and provided evidence that these two COLs and HY5 were connected together to form an HY5-COL3-COL13 regulatory chain that controls hypocotyl elongation in *Arabidopsis* (Fig. 7b). In addition, we also proposed a possible COP1-dependent COL3-COL13 feedback pathway, to optimize this regulatory pathway (Fig. 7b).

Hypocotyl elongation is a genetically well-controlled process to response the light. In *Arabidopsis* , several key genes are required for hypocotyl growth. Among these, COP1 is a negative regulator (McNellis, von Arnim, & Deng, 1994), while HY5 and COL3 are considered to be positive ones (Datta et al., 2006; Hardtke et al., 2000). A previous study showed that COL3 played roles in flowering and hypocotyl elongation (Datta et al.,

2006), and COL3 is known to interact with B-BOX32 to regulate flowering (Tripathi et al., 2017). However, there has no research on how COL3 regulates hypocotyl elongation. To explore how the COL family genes, COL3 in particular, function in the regulation of hypocotyl elongation will be facilitated by identifying the downstream genes. In this study, we demonstrated that *COL13*, whose RNA accumulated to high level in hypocotyl (Fig.1), was one more positive regulator in the regulation of hypocotyl elongation under red light conditions. For example, overexpression of *COL13* or knock down its transcript resulted in a shorter or longer hypocotyl, respectively (Fig. 2). To further define and characterize *COL13*, we analyzed genetic interactions between *col13* and *col3*. Seedlings of the *col13* and *col3* mutants showed reduced inhibition of hypocotyl elongation in red light (Fig.3). Analysis of *col3 col13* double mutants and *COL13* transgenic plants revealed that *COL3* is epistatic to *COL13* with respect to hypocotyl elongation (Fig. 3). Given that *col3 hy5* double mutants behaved like the *hy5* mutation (Datta et al., 2006), we hypothesized that there is a HY5-COL3-COL13 regulatory chain for controlling hypocotyl growth. As expected, our data proved that HY5 directly targeted the promoter of *COL3* and COL3 directly bound to the promoter of *COL13* (Fig. 4a-c), indicating that HY5, COL3 and COL13 constitute a hypocotyl regulatory pathway.

CONSTANS-LIKE genes belong to BBX family. Given that BBX family members are commonly involved in photomorphogenesis and that they can interact with other BBX proteins to regulate plant growth (Tripathi et al., 2017; Wang et al., 2014), it is possible that COL3 interacts with other BBX proteins (eg. COL13/B-BOX11) to regulate plant development in light. Indeed, we provided evidence that COL13 can interact with COL3 (Fig. 6). Furthermore, we found that the expression of COL13 promoted the interaction between COP1 and COL3 (Fig. 7a). To our knowledge, COP1 is responsible for degradation of several positive transcription factors such as COL3 in the dark (Datta et al., 2006; Dornan et al., 2004; Duek et al., 2004; Lau & Deng, 2012; Osterlund et al., 2000; Seo et al., 2004; Seo et al., 2003). Increasing the bind activity of COP1 and COL3 would lead to the degradation of COL3. As a result, there would be less COL3 to active the expression of COL13 (Fig. 7b). The COP1-dependent COL3-COL13 feedback pathway could enrich the regulation network in hypocotyl elongation.

## Acknowledgements

We are grateful to Prof. Magnus Holm (Gothenburg University, Sweden) for providing *col3* mutant seeds. This work was supported by the National Natural Science Foundation of China (31572161 and 31672188), the Youth Foundation of the National Natural Science Foundation of China (30900107) and China International Postdoctoral Program.

## References

- Ang, L.-H., Chattopadhyay, S., Wei, N., Oyama, T., Okada, K., Batschauer, A., & Deng, X.-W. (1998). Molecular interaction between COP1 and HY5 defines a regulatory switch for light control of Arabidopsis development. *Molecular cell*, 1 (2), 213-222.
- Cheng, X. F., & Wang, Z. Y. (2005). Overexpression of COL9, a CONSTANS-LIKE gene, delays flowering by reducing expression of CO and FT in Arabidopsis thaliana. *The Plant Journal*, 43 (5), 758-768.
- Clough, S. J., & Bent, A. F. (1998). Floral dip: a simplified method for Agrobacterium-mediated transformation of Arabidopsis thaliana. *The Plant Journal*, 16 (6), 735-743.
- Crocco, C. D., Holm, M., Yanovsky, M. J., & Botto, J. F. (2010). AtBBX21 and COP1 genetically interact in the regulation of shade avoidance. *The Plant Journal*, 64 (4), 551-562.
- Crocco, C. D., Locascio, A., Escudero, C. M., Alabadí, D., Blázquez, M. A., & Botto, J. F. (2015). The transcriptional regulator BBX24 impairs DELLA activity to promote shade avoidance in Arabidopsis thaliana. *Nature communications*, 6, 6202.
- Datta, S., Hettiarachchi, G., Deng, X.-W., & Holm, M. (2006). Arabidopsis CONSTANS-LIKE3 is a positive regulator of red light signaling and root growth. *The plant cell*, 18 (1), 70-84.

Delker, C., Sonntag, L., James, G. V., Janitza, P., Ibañez, C., Ziermann, H., . . . Ziegler, J. (2014). The DET1-COP1-HY5 pathway constitutes a multipurpose signaling module regulating plant photomorphogenesis and thermomorphogenesis. *Cell Reports*, *9* (6), 1983-1989.

Dornan, D., Wertz, I., Shimizu, H., Arnott, D., Frantz, G. D., Dowd, P., . . . Dixit, V. M. (2004). The ubiquitin ligase COP1 is a critical negative regulator of p53. *Nature*, *429* (6987), 86.

Duek, P. D., Elmer, M. V., van Oosten, V. R., & Fankhauser, C. (2004). The degradation of HFR1, a putative bHLH class transcription factor involved in light signaling, is regulated by phosphorylation and requires COP1. *Current Biology*, *14* (24), 2296-2301.

Fiil, B. K., Qiu, J.-L., Petersen, K., Petersen, M., & Mundy, J. (2008). Coimmunoprecipitation (co-IP) of nuclear proteins and chromatin immunoprecipitation (ChIP) from Arabidopsis. *Cold Spring Harbor Protocols*, *2008* (9), pdb. prot5049.

Gangappa, S. N., Crocco, C. D., Johansson, H., Datta, S., Hettiarachchi, C., Holm, M., & Botto, J. F. (2013). The Arabidopsis B-BOX protein BBX25 interacts with HY5, negatively regulating BBX22 expression to suppress seedling photomorphogenesis. *The plant cell*, *25* (4), 1243-1257.

Graeff, M., Straub, D., Eguen, T., Dolde, U., Rodrigues, V., Brandt, R., & Wenkel, S. (2016). MicroProtein-mediated recruitment of CONSTANS into a TOPLESS trimeric complex represses flowering in Arabidopsis. *PLoS genetics*, *12* (3), e1005959.

Han, M., Jin, X., Yao, W., Kong, L., Huang, G., Tao, Y., . . . Wang, Y. (2017). A Mini Zinc-Finger Protein (MIF) from *Gerbera hybrida* Activates the GASA Protein Family Gene, GEG, to Inhibit Ray Petal Elongation. *Frontiers in plant science*, *8*, 1649.

Hardtke, C. S., Gohda, K., Osterlund, M. T., Oyama, T., Okada, K., & Deng, X. W. (2000). HY5 stability and activity in Arabidopsis is regulated by phosphorylation in its COP1 binding domain. *The EMBO journal*, *19* (18), 4997-5006.

Hou, K., Wu, W., & Gan, S.-S. (2013). SAUR36, a small auxin up RNA gene, is involved in the promotion of leaf senescence in Arabidopsis. *Plant Physiology*, *161* (2), 1002-1009.

Josse, E.-M., & Halliday, K. J. (2008). Skotomorphogenesis: the dark side of light signalling. *Current Biology*, *18* (24), R1144-R1146.

Kami, C., Lorrain, S., Hornitschek, P., & Fankhauser, C. (2010). Light-regulated plant growth and development. In *Current topics in developmental biology* (Vol. 91, pp. 29-66): Elsevier.

Khanna, R., Kronmiller, B., Maszle, D. R., Coupland, G., Holm, M., Mizuno, T., & Wu, S.-H. (2009). The Arabidopsis B-box zinc finger family. *The plant cell*, *21* (11), 3416-3420.

Kircher, S., Gil, P., Kozma-Bognár, L., Fejes, E., Speth, V., Husselstein-Muller, T., . . . Nagy, F. (2002). Nucleocytoplasmic partitioning of the plant photoreceptors phytochrome A, B, C, D, and E is regulated differentially by light and exhibits a diurnal rhythm. *The plant cell*, *14* (7), 1541-1555.

Klepikova, A. V., Kasianov, A. S., Gerasimov, E. S., Logacheva, M. D., & Penin, A. A. (2016). A high resolution map of the Arabidopsis thaliana developmental transcriptome based on RNA-seq profiling. *The Plant Journal*, *88* (6), 1058-1070.

Kumagai, T., Ito, S., Nakamichi, N., Niwa, Y., Murakami, M., Yamashino, T., & Mizuno, T. (2008). The common function of a novel subfamily of B-Box zinc finger proteins with reference to circadian-associated events in Arabidopsis thaliana. *Bioscience, Biotechnology, and Biochemistry*, *72* (6), 1539-1549.

Lau, O. S., & Deng, X. W. (2012). The photomorphogenic repressors COP1 and DET1: 20 years later. *Trends in plant science*, *17* (10), 584-593.

- Lee, H.-J., Park, Y.-J., Ha, J.-H., Baldwin, I. T., & Park, C.-M. (2017). Multiple routes of light signaling during root photomorphogenesis. *Trends in plant science*, *22* (9), 803-812.
- Lee, J., He, K., Stolc, V., Lee, H., Figueroa, P., Gao, Y., . . . Deng, X. W. (2007). Analysis of transcription factor HY5 genomic binding sites revealed its hierarchical role in light regulation of development. *The plant cell*, *19* (3), 731-749.
- Li, F., Sun, J., Wang, D., Bai, S., Clarke, A. K., & Holm, M. (2014). The B-box family gene STO (BBX24) in *Arabidopsis thaliana* regulates flowering time in different pathways. *PloS one*, *9* (2), e87544.
- Liu, B., Liu, X., Yang, S., Chen, C., Xue, S., Cai, Y., . . . Ren, H. (2016). Silencing of the gibberellin receptor homolog, CsGID1a, affects locule formation in cucumber (*Cucumis sativus*) fruit. *New Phytologist*, *210* (2), 551-563.
- Liu, Y., Lai, J., Yu, M., Wang, F., Zhang, J., Jiang, J., . . . Xu, P. (2016). The *Arabidopsis* SUMO E3 ligase AtMMS21 dissociates the E2Fa/DPa complex in cell cycle regulation. *The plant cell*, 00439.02016.
- McNellis, T. W., & Deng, X.-W. (1995). Light control of seedling morphogenetic pattern. *The plant cell*, *7* (11), 1749.
- McNellis, T. W., von Arnim, A. G., & Deng, X.-W. (1994). Overexpression of *Arabidopsis* COP1 results in partial suppression of light-mediated development: evidence for a light-inactivable repressor of photomorphogenesis. *The plant cell*, *6* (10), 1391-1400.
- Muntha, S. T., Zhang, L., Zhou, Y., Zhao, X., Hu, Z., Yang, J., & Zhang, M. (2018). Phytochrome A signal transduction 1 and CONSTANS-LIKE 13 coordinately orchestrate shoot branching and flowering in leafy *Brassica juncea*. *Plant biotechnology journal*.
- Olle, M., & Viršile, A. (2013). The effects of light-emitting diode lighting on greenhouse plant growth and quality. *Agricultural and food science*, *22* (2), 223-234.
- Osterlund, M. T., Hardtke, C. S., Wei, N., & Deng, X. W. (2000). Targeted destabilization of HY5 during light-regulated development of *Arabidopsis*. *Nature*, *405* (6785), 462.
- Park, H.-Y., Lee, S.-Y., Seok, H.-Y., Kim, S.-H., Sung, Z. R., & Moon, Y.-H. (2011). EMF1 interacts with EIP1, EIP6 or EIP9 involved in the regulation of flowering time in *Arabidopsis*. *Plant and cell physiology*, *52* (8), 1376-1388.
- Preuss, S. B., Meister, R., Xu, Q., Urwin, C. P., Tripodi, F. A., Screen, S. E., . . . Liu, G. (2012). Expression of the *Arabidopsis thaliana* BBX32 gene in soybean increases grain yield. *PloS one*, *7* (2), e30717.
- Putterill, J., Robson, F., Lee, K., Simon, R., & Coupland, G. (1995). The CONSTANS gene of *Arabidopsis* promotes flowering and encodes a protein showing similarities to zinc finger transcription factors. *cell*, *80* (6), 847-857.
- Quail, P. H. (2002). Phytochrome photosensory signalling networks. *Nature reviews Molecular cell biology*, *3* (2), 85.
- Quail, P. H. (2002). Phytochrome photosensory signalling networks. *Nature Reviews Molecular Cell Biology*, *3* (2), 85-93.
- Robson, F., Costa, M. M. R., Hepworth, S. R., Vizir, I., Pinheiro, M., Reeves, P. H., . . . Coupland, G. (2001). Functional importance of conserved domains in the flowering-time gene CONSTANS demonstrated by analysis of mutant alleles and transgenic plants. *The Plant Journal*, *28* (6), 619-631.
- Rosso, M. G., Li, Y., Strizhov, N., Reiss, B., Dekker, K., & Weisshaar, B. (2003). An *Arabidopsis thaliana* T-DNA mutagenized population (GABI-Kat) for flanking sequence tag-based reverse genetics. *Plant molecular biology*, *53* (1-2), 247-259.

Seo, H. S., Watanabe, E., Tokutomi, S., Nagatani, A., & Chua, N.-H. (2004). Photoreceptor ubiquitination by COP1 E3 ligase desensitizes phytochrome A signaling. *Genes & development*, *18* (6), 617-622.

Seo, H. S., Yang, J.-Y., Ishikawa, M., Bolle, C., Ballesteros, M. L., & Chua, N.-H. (2003). LAF1 ubiquitination by COP1 controls photomorphogenesis and is stimulated by SPA1. *Nature*, *423* (6943), 995.

Smith, H. (2000). Phytochromes and light signal perception by plants—an emerging synthesis. *Nature*, *407* (6804), 585.

Tripathi, P., Carvallo, M., Hamilton, E. E., Preuss, S., & Kay, S. A. (2017). Arabidopsis B-BOX32 interacts with CONSTANS-LIKE3 to regulate flowering. *Proceedings of the National Academy of Sciences*, *114* (1), 172-177.

von Arnim, A. G., & Deng, X.-W. (1994). Light inactivation of Arabidopsis photomorphogenic repressor COP1 involves a cell-specific regulation of its nucleocytoplasmic partitioning. *cell*, *79* (6), 1035-1045.

Wang, C.-Q., Guthrie, C., Sarmast, M. K., & Dehesh, K. (2014). BBX19 interacts with CONSTANS to repress FLOWERING LOCUS T transcription, defining a flowering time checkpoint in Arabidopsis. *The plant cell*, tpc. 114.130252.

Wu, F.-H., Shen, S.-C., Lee, L.-Y., Lee, S.-H., Chan, M.-T., & Lin, C.-S. (2009). Tape-Arabidopsis Sandwich—a simpler Arabidopsis protoplast isolation method. *Plant methods*, *5* (1), 16.

Wu, G., Cameron, J. N., Ljung, K., & Spalding, E. P. (2010). A role for ABCB19-mediated polar auxin transport in seedling photomorphogenesis mediated by cryptochrome 1 and phytochrome B. *The Plant Journal*, *62* (2), 179-191.

Xu, D., Jiang, Y., Li, J., Holm, M., & Deng, X. W. (2018). The B-box domain protein BBX21 promotes photomorphogenesis. *Plant Physiology*, *176* (3), 2365-2375.

Xu, D., Jiang, Y., Li, J., Lin, F., Holm, M., & Deng, X. W. (2016). BBX21, an Arabidopsis B-box protein, directly activates HY5 and is targeted by COP1 for 26S proteasome-mediated degradation. *Proceedings of the National Academy of Sciences*, 201607687.

Yang, Y., Ma, C., Xu, Y., Wei, Q., Imtiaz, M., Lan, H., . . . Fei, Z. (2014). A zinc finger protein regulates flowering time and abiotic stress tolerance in chrysanthemum by modulating gibberellin biosynthesis. *The plant cell*, tpc. 114.124867.

Zhang, Y., Liu, B., Yang, S., An, J., Chen, C., Zhang, X., & Ren, H. (2014). A cucumber DELLA homolog CsGAIP may inhibit staminate development through transcriptional repression of B class floral homeotic genes. *PLoS one*, *9* (3), e91804.

Zhang, Y., Zhang, X., Liu, B., Wang, W., Liu, X., Chen, C., . . . Ren, H. (2014). A GAMYB homologue CsGAMYB1 regulates sex expression of cucumber via an ethylene-independent pathway. *Journal of experimental botany*, *65* (12), 3201-3213.

### Author contributions

S.S. and W.X. proposed the project. S.S., W.X. and L.B. designed the experiments. L.B., L.H., Y.J., Y.L., Z.Q., C.H. and G.S. performed the experiments. L.B. and S.S. analyzed the data, L.B. wrote the manuscript, with the participation of S.S. and W.Y.

### Figure legends

**Fig.1 COL13 RNA accumulates to high levels in hypocotyl.** (a) Quantitative real time-PCR analysis of AtCOL13 transcript abundance in different tissues. R=Root, S=Stem, L=Leaf, SAM=Shoot apical meristem, H=Hypocotyl, F=Flower. (b) Activity of COL13 promoter revealed by  $\beta$ -glucuronidase (GUS) staining in Arabidopsis seedlings. Bar=100 mm.

**Fig.2 COL13 regulates hypocotyl elongation under red-light conditions.** (a) Relative expression of COL13 in Col-0 and overexpression (OX) lines. (b) Relative expression of COL13 in Col-0, T-DNA mutant (*col13*) and RNAi lines (R1-1 etc.). (c)-(e) Phenotypic analysis seedlings of the indicated genotypes were grown in the presence of red light. Images of representative seedlings are shown in (c). The hypocotyl lengths of the indicated genotypes were measured and are shown in (d) and (e). Error bars indicate SD (n >15). Asterisks indicate that hypocotyl lengths in OX9 and *col13*, COL13 RNAi are significantly different with WT under red light (P < 0.05).

**Fig. 3 Genetic interaction and physiological characterization of hypocotyl elongation.** (a) Semi-quantitative RT-PCR analyses of COL13 expression in *phyB*, *col3*, *hy5* and *cop1* mutants. (b) qRT-PCR analyses of COL13 expression in *phyB*, *col3*, *hy5* and *cop1* mutants. (c) Activity of the COL13 promoter revealed by  $\beta$ -glucuronidase (GUS) staining in WT and *col3* mutant backgrounds. (d) Hypocotyl length in WT, single- and double-mutant plants. (e) Hypocotyl length in WT and *col3* plants compared to transgenic plants with COL13 RNAi or COL13 overexpression (OX) in the *col3* background. Error bars indicate SD (n >15). Lower-case letters indicate significantly different data groups (hypocotyl length) of the indicated seedlings grown in red light.

**Fig.4 Analysis of the binding of HY5 to COL3 promoter, and COL3 to COL13 promoter truncations.** (a) Diagram of constructs used. The AD-HY5 or AD-COL3 fusion gene driven by the 35S promoter produces a potential effector protein, while the AD protein alone represents a negative control for basal activity of COL3 promoter or each COL13 promoter truncation. The LUC gene driven by the series of COL3 promoter or COL13 promoter truncations tests the ability of the AD-HY5 or AD-COL3 fusion protein to bind to each promoter truncation. (b) The fusion protein AD-HY5, but not AD alone, can effect LUC expression from the COL3 promoter truncations, and the fusion protein AD-COL3, but not AD alone, can effect LUC expression from some of the COL13 promoter truncations. (c) Electrophoretic mobility shift assay (EMSA) analysis showing the binding of COL3 to COL13 the -1421 to -1184 bp promoter (probe 2) in vitro. The black arrow indicates binding of COL3 to the biotin-labeled COL13 promoter. The + and - represent the presence and absence of corresponding components, respectively.

**Fig.5 Subcellular localization of COL13.** (a) COL13-CFP localizes to the nucleus in protoplasts. (d) COL13-GFP localizes to the nucleus in root tip cells.

**Fig.6 COL13 interacts with COL3.** (a) Yeast Two-Hybrid assay between COL13 and COL3. DDO, Double Dropout; QDO, Quadruple Dropout; pGADT7, prey plasmid; pGBKT7, bait plasmid. (b) Co-immunoprecipitation (Co-IP) in Arabidopsis. Immunoprecipitations (IPs) were performed on protein extracted from 10-d-old Arabidopsis seedlings grown under long-day illumination (16L: 8D) at 22°C. Leaf tissues were harvested 1 h after the light cycle commenced. IP was performed using anti-HA antibody and COL13 was co-immunoprecipitated with anti-GFP antibody. A 5% input was used. Western blots were performed on 10% (wt/vol) precast gels (Bio-Rad). (c) COL3-CFP and COL13-YFP colocalize to the nucleus in protoplasts in light and dark. (d-f) FRET between CFP-COL3 and YFP-COL13 analyzed by acceptor bleaching in the nucleus. The top panels in (d) show a representative pre-bleach nucleus coexpressing YFP-COL13 and CFP-COL3 excited with either a 514- or a 405-nm laser in light and dark, resulting in emission from YFP (yellow) or CFP (blue), respectively. The bottom panels in (d) show the same nucleus post-bleaching after excitation with a 514- or a 405-nm laser. The relative intensities of both YFP and CFP were measured before and after bleaching, as indicated in (e) and (f).

**Fig.7 COL13 promotes the interaction between COL3 and COP1.** (a) Yeast three-hybrid analysis of the COP1-COL3 interaction in the presence of COL13. Normalized Miller Units were calculated as a ratio of  $\alpha$ -galactosidase activity in yeast. Additionally, normalized Miller Units here are reported separately for yeast grown on media without or with 1 mM methionine (Met), corresponding to induction (-Met) or repression (+Met) of Met25 promoter-driven COL13 expression, respectively. Means and SEM for three biological repetitions are shown. Lower-case letters indicate significant difference of  $\alpha$ -galactosidase. (b) A model representing the HY5-COL3-COL13 regulatory chain and COP1-dependent COL3-COL13 feedback pathway in regulation of hypocotyl elongation.

## Supporting Information

**Table S1** List of primers and their uses.

**Table S2** Probes used in EMSA assay

**Fig.S1 COL13 regulates hypocotyl elongation under red-light conditions.** (a) Scheme of the Arabidopsis COL13 gene (AT2G47890) showing the T-DNA insertion position. (b) Identification of the sulfonamide resistance gene (SUL) in the *col13* mutant by PCR. (c) The hypocotyl lengths of wild type (WT), COL13 RNAi and *col13* seedlings under different light condition. Error bars indicate SD ( $n > 15$ ). Lower-case letters indicate significantly difference ( $P < 0.05$ ).

**Fig. S2** Electrophoretic mobility shift assay (EMSA) showing binding of COL3 to the COL13 promoter in vitro.

**Fig. S3 COP1 can interact with COL3, but not COL13.** a COL3-CFP and COP1-YFP co-localize to the nucleus in protoplasts in both light and dark conditions. b FRET between CFP-COL3 and YFP-COP1 analyzed by acceptor bleaching in the nucleus. The top panels in b show a representative pre-bleach nucleus coexpressing YFP-COP1 and CFP-COL3 excited with either a 514- or a 405-nm laser in light and dark, resulting in emission from YFP (yellow) or CFP (blue), respectively. The bottom panels in b show the same nucleus after bleaching following excitation with a 514- or a 405-nm laser. The relative intensities of both YFP and CFP were measured once before and twice after bleaching, as indicated in c and d. e COL13-CFP and COP1-YFP co-localize to the nucleus in protoplasts in light and dark. f FRET between CFP-COL13 and YFP-COP1 analyzed by acceptor bleaching in the nucleus. The top panels in f show a representative pre-bleach nucleus co-expressing YFP-COP1 and CFP-COL13 excited with either a 514- or a 405-nm laser in light and dark, resulting in emission from YFP (yellow) or CFP (blue), respectively. The bottom panels in f show the same nucleus after bleaching following excitation with a 514- or a 405-nm laser. The relative intensities of both YFP and CFP were measured once before and twice after bleaching, as indicated in g and h.

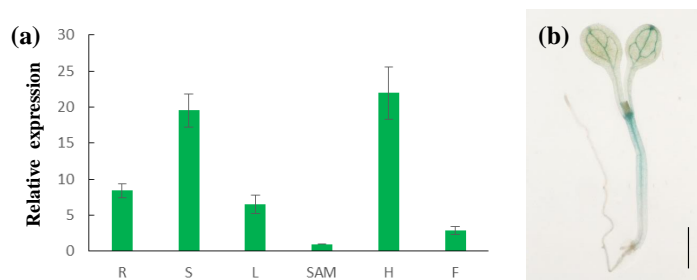


**Fig.1 COL13 RNA accumulates to high levels in hypocotyl.** (a) Quantitative real time-PCR analysis of *AtCOL13* transcript abundance in different tissues. R=Root, S=Stem, L=Leaf, SAM=Shoot apical meristem, H=Hypocotyl, F=Flower. (b) Activity of *COL13* promoter revealed by  $\beta$ -glucuronidase (GUS) staining in Arabidopsis seedlings. Bar=100 mm.